C. R. Mecanique 342 (2014) 52–62

Contents lists available at ScienceDirect

Comptes Rendus Mecanique

www.sciencedirect.com

Wavelength selection of ripples in a vertically vibrating dynamically thick granular layer due to density-wave refraction ☆

Osamu Sano

Department of Applied Physics, Tokyo University of Agriculture & Technology, Tokyo 184-8588, Japan

ARTICLE INFO

Article history:
Received 10 July 2013
Accepted 15 October 2013
Available online 1 January 2014

Keywords:
Granular material
Dynamically thick layer
Density wave
Refraction
Wavelength
Solid–fluid transition

ABSTRACT

A numerical study was made on the wavelength selection mechanism of the ripples observed on the surface of a granular layer that is oscillated vertically. Multiple collisions of the one-dimensional array of beads show a time-dependent particle distribution, which induces a density wave. The magnitude of the wave velocity is estimated by the theory of elasticity, which reveals the refraction of the density wave in a quasi-two-dimensional granular layer. Our theory explains how the vertical excitation of particles determines the horizontal characteristic scale on the surface, or the wavelength of the ripples, which is applicable even to the saturation regime of a dynamically thick granular layer, e.g., the one that is thick enough to allow an immobilized region in the lower part.

1. Introduction

It is well known that a vertically vibrating granular layer shows typical wave motions called *undulations* and *ripples* depending on the amplitude a and frequency f of the external forcing [1–5]. The formation of undulation has been examined [6–13], in which buckling due to the dilatancy of the layer at the collision of the bottom wall is found to be the fundamental mechanism. Here the layer behaves like an elastic plate. Note that the buckling due to the dilatancy of the layer can occur for a layer number (i.e., thickness relative to particle diameter) larger than about 3 [11,12] (disappearance of the waves for the layer as small as 3 particle diameters thick has long been remarked [14,15]). On the other hand, the same material shows a fluid-like behavior under certain external forcing, and the parametrically excited surface waves with frequency $f/2, f/4, \ldots$ are generated. The latter is exemplified by the surface waves viewed in the vertical cross-section [15–19], and the surface waves viewed from above [14,20–26].

The wavelength selection mechanism, however, seems a little complicated. In a thin granular layer where the whole region is fluidized, a fluid mechanical analogy, and hence the dispersion relation for the gravity wave will be appropriate, as are proposed by the above-mentioned papers. Phenomenological theories assuming continuum models [27–30], as well as fluid dynamical stability analyses [31,32] are also proposed. In spite of these studies, a lot of different dispersion relations are proposed. The latter discrepancy seems to stem from different choices of particles and different aspect ratios of the granular layer, among others. A closer look at the wave motion using the same species of particles reveals that the dispersion relation based on the layer thickness h deviates considerably from that obtained by the continuum model with the increase of h. The wavelength λ looks saturated above a certain layer thickness h^* [14,15,18,19], the value of which may depend on

☆ The paper was presented in the mini-symposium about "Recent Advances in the Mechanics of Granular and Porous Media" at the European Solid Mechanics Conference 2012 in Graz, Austria. The guest editors of this Mini-Symposium are Erich Bauer, Robert P. Behringer, Félix Darve and Lou Kondic.

E-mail address: sano@cc.tuat.ac.jp.

1631-0721/$ – see front matter
http://dx.doi.org/10.1016/j.crme.2013.10.006

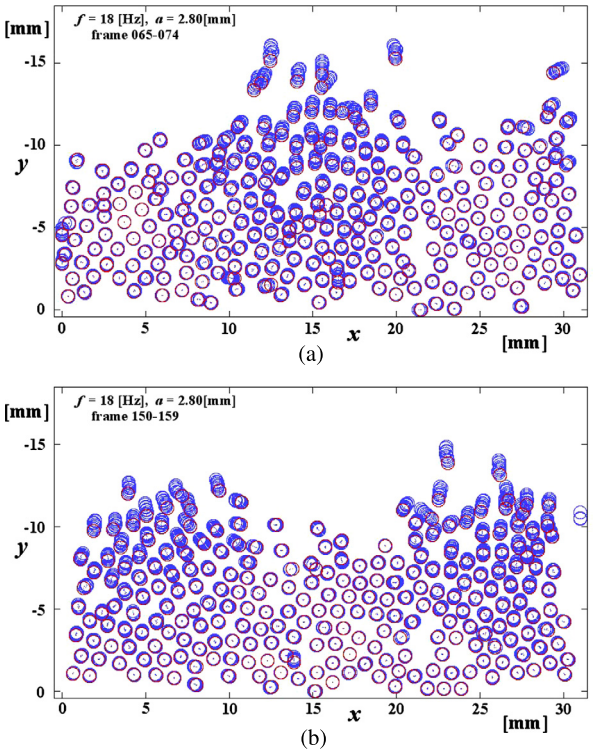

Fig. 1. (Color online.) Solid–fluid transition in vertically vibrating granular layer ($f = 18$ Hz, $a = 2.8$ mm).

the properties of the particle as well as on the external forcing condition. This suggests that the total layer thickness h is not always a good measure of the dispersion relation. Indeed, non-uniform fluidization in dynamically thick layers has been remarked in the cellular pattern formation [26] and 2D ripples in a vertical cell [41,42]. The former proposed the horizontal grain mobility transition in their study on the wavelength scaling in the planar patterns, where grains are essentially mobile or immobile according to whether they are above or below the critical state, but non-uniform particle distribution was not explicitly shown. On the other hand, the latter papers revealed that some part of the particles do not change their relative positions over the distance larger than a particle diameter distance, which is regarded as a "solid" or elastic state. The solid and the fluid regions coexist in deep beds of granular material, and they change spatiotemporally with the external forcing. In summary, a vertically vibrating granular layer is characterized by the fluid-like ripples under the following conditions: (i) the layer number is larger than about 3 and (ii) the layer thickness is smaller than a certain value h^* (or a certain layer number N^*) where saturation of the dispersion relation sets in. Throughout this paper, we denote the *dynamically thick* layer whose thickness is larger than h^*. At first thought, a macroscopic continuum description will better be adapted to larger numbers of particles, which is not the case in granular layers, mainly because of the non-negligible effect of dissipation, and hence of the non-uniform distribution of the particles. Then a question arises on how the wavelength is determined in vibrating dynamically thick layers.

The presence and the spatiotemporal change of the particle number density distribution under a certain external vibration have already been treated in different situations. Indeed, the vertical propagation of the shock wave in vertically vibrated granular layers [33–35], as well as the propagation of a kink in horizontal layers [36,37], reveals the spatiotemporal change of particle configuration inside the granular material. In the granular surface waves, some qualitative descriptions [26,38] or 3D numerical simulation by means of DEM [39] have also been made, but they do not explicitly refer to the surface wave formation mechanism. It is quite recently that the experimental evidence of the motion of the constituent particle was provided [40–42]. Fig. 1 shows ripples in ten layers of lead spheres of a diameter $d = 1.0$ mm. In each figure, ten images during 4.5 ms are superposed. Particles where open circles are recognized show no relative motion with respect to each other, which corresponds to the immobilized domain, whereas circles of varied centers show a fluid domain. In the example shown, the wave pattern repeats at every 111 ms (reflecting a parametric oscillation of period $2/f$ s), and Fig. 1(b) is the one 42.5 ms after that of Fig. 1(a). A closer look at the experiment reveals that the type of motion of the constituent particles is not the same throughout the layer. Both solid-like and fluid-like domains coexist in dynamically thick layers, and their positions and sizes are repeatedly changing, whose boundaries propagate as a density wave. It is only the upper fluid-like region that is relevant to the ripple formation. Although the solid-like layer looks thin in Fig. 1, the presence of a much thicker solid-like layer is recognized for larger layer numbers, as shown in Ref. [41].

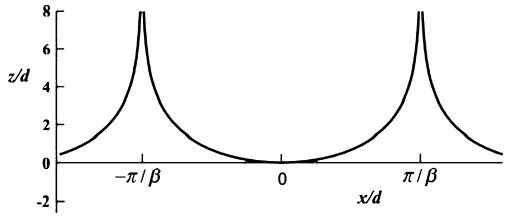

Fig. 2. Wavelength selection of the ripples: a "ray" of the density wave.

Taking into account our experimental findings, we have recently developed a new theory on the determination of the wavelength of ripples in vertically vibrating dynamically thick granular layers [41,42]. We assume that the velocity v of the density wave depends on the positions, which reflects the extent of particle compaction. When the layer collides with the bottom wall, the compacted region develops in the vertical direction, which accompanies particle displacement in the horizontal direction due to dilatancy, and hence induces the non-uniform propagation of the density wave. The refraction of such a wave can be described by the "ray" theory. For example, when the propagation velocity v varies vertically as $v = v_0 \exp(-\beta z/(2d))$ (β being a constant, and v_0 a certain reference velocity), the trajectory of the ray is given by [50]:

$$\frac{z}{d} = -\frac{2}{\beta}\log\left|\cos\left[\frac{\beta}{2d}(x - x_0)\right]\right| \tag{1}$$

where z is the vertical position, x is the horizontal coordinate, and x_0 is a certain reference position. In this model, the wavelength λ is given by:

$$\lambda = \frac{2\pi d}{\beta} \tag{2}$$

as shown in Fig. 2. Note that the above-mentioned velocity distribution can be an approximate one near the layer surface. If the velocity distribution is constant in the lower compacted region, the density wave will propagate uniformly in that region, so that the latter region will have no contribution to the ripple formation. The applicability to a granular layer of any thickness is one of the advantage of our theory, which should be checked.

The constant β characterizes the dilatation of the layer, and is related to the external forcing f, a and phase ϕ, as well as the properties of the material like restitution coefficient e, friction μ, and so on. In order to obtain the dependence of β on these properties, we performed a simple numerical simulation, where collisions of a one-dimensional column of identical spheres were examined [43]. The latter takes into account f, a and e, but the layer number N was fixed. In contrast to extending the present model to a 2D or 3D configuration of particles, which might better be made by direct numerical simulations (e.g., Ref. [39]), we are much more concerned with the mechanism on how the vertical excitation of particles determines the horizontal characteristic scale on the surface. Whether or not our simple 1D model [43] is appropriate should better be tested in dynamically thick layers accompanied by the layer height saturation, which compels us to examine the dependence of the layer number N on the ripple formation.

2. Numerical simulation

In order to ascertain whether the present 1D column model is valid as a mechanism for determining the wavelength even in the presence of a lower immobilized part of the layer, we shall perform a numerical simulation, assuming a one-dimensional (1D) array of N hard spheres of equal diameter d and equal mass, which is excited vertically by the sinusoidal oscillation of the bottom plate with amplitude a and frequency $f(\equiv \omega/(2\pi))$, such that $z_0 = a\sin(2\pi f t)$. We denote the position of the center of the i-th particle by z_i $(i = 1, \ldots, N)$ and the position of the plate by z_0. The relations between the velocities of the plate and particles before the collision $(v_0, v_1, \ldots, v_N)$ and those after the collision $(u_0, u_1, \ldots, u_N)$ are:

$$\begin{pmatrix} u_0 \\ u_1 \end{pmatrix} = \begin{pmatrix} 1 & 0 \\ 1+e' & -e' \end{pmatrix} \begin{pmatrix} v_0 \\ v_1 \end{pmatrix} \tag{3}$$

$$\begin{pmatrix} u_{i-1} \\ u_i \end{pmatrix} = \frac{1}{2}\begin{pmatrix} 1-e & 1+e \\ 1+e & 1-e \end{pmatrix} \begin{pmatrix} v_{i-1} \\ v_i \end{pmatrix}, \quad i = 2, \ldots, N \tag{4}$$

where e is the restitution coefficient between the particles and e' is that between the particle and the plate, which are assumed constant for simplicity. We also neglected the friction due to air viscosity. In the simulation, we have chosen the particle mass m, its size d and the acceleration of gravity g as units, so that the frequency and amplitude of the external forcing are scaled by $\sqrt{g/d}$ and d, respectively.

In contrast to the previous calculations, where collapse or clustering of granular gasses [44–46] and the mean dilatation of the column of beads [47–49] were focused, we have recalculated the multi-collisional process with the intention of obtaining the vertical distribution of divergence $\Delta(z)$, because it is this property that determines the refraction of the wave.

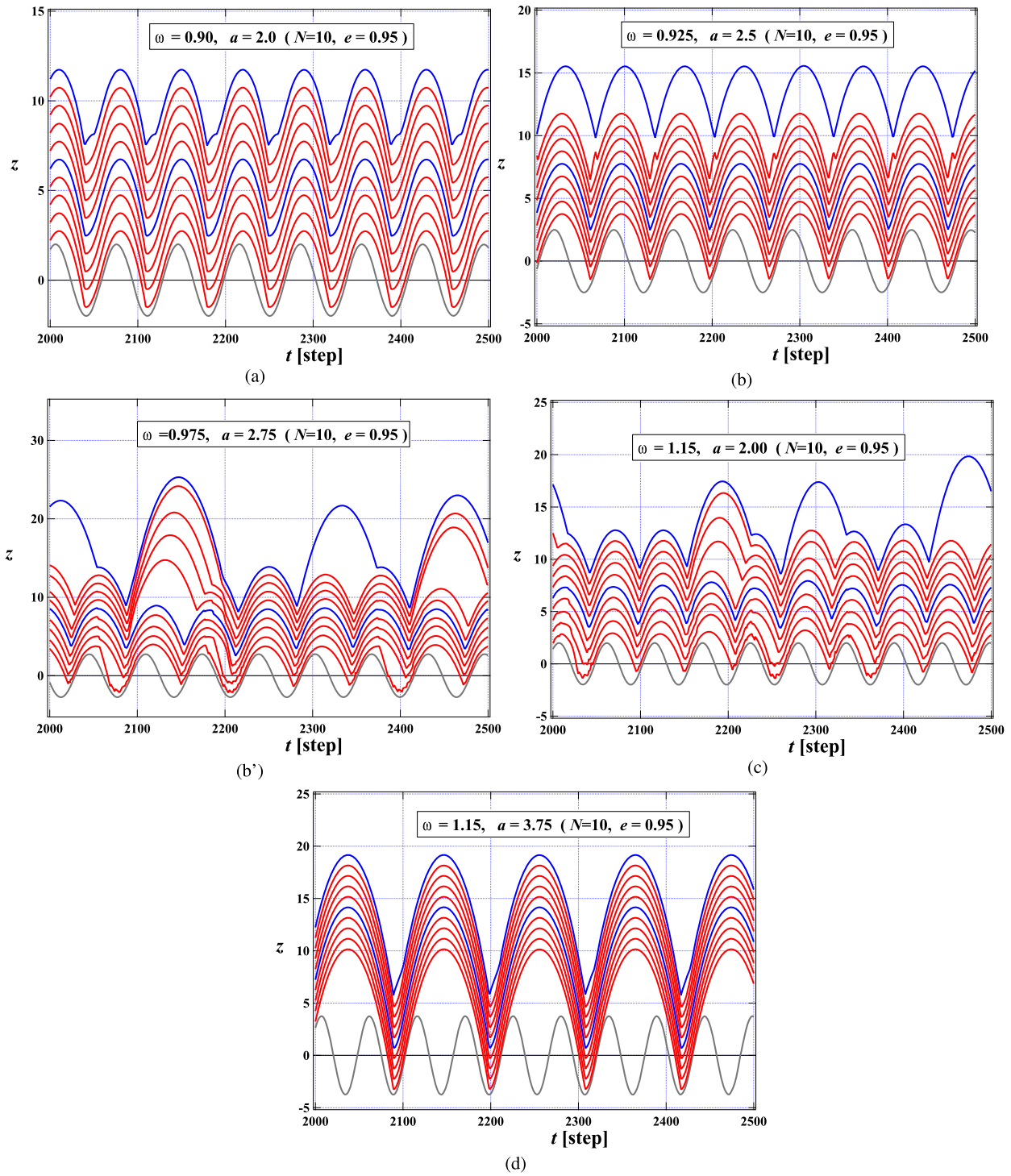

Fig. 3. (Color online.) Particle behavior for $N = 10$; (ω, a) = (a) (0.900, 2.00), (b) (0.925, 2.50), (b′) (0.975, 2.75), (c) (1.150, 2.00), (d) (1.150, 3.75), (e) (1.200, 4.00), and (e′) (1.100, 4.50). In (a) and (d), the particle motion is regular, and no ripples are expected. In (b), (c) and (d), the lower part of the layer is almost solid-like, but the dilatation looks larger in the upper layers. Separation of the layer in the middle part is recognized in (e).

We calculated the average positions $\bar{z}_i$ $(i = 1, 2, \ldots, N)$ and their standard deviations, the latter of which are regarded as Δ. According to the theory of elasticity [50], the velocity v and pressure p in the material with the effective bulk modulus K^* and the effective density ρ^* are given by $v = \sqrt{K^*/\rho^*}$ and $p = -K^*\Delta$. In an ordinary granular material, a local equilibrium

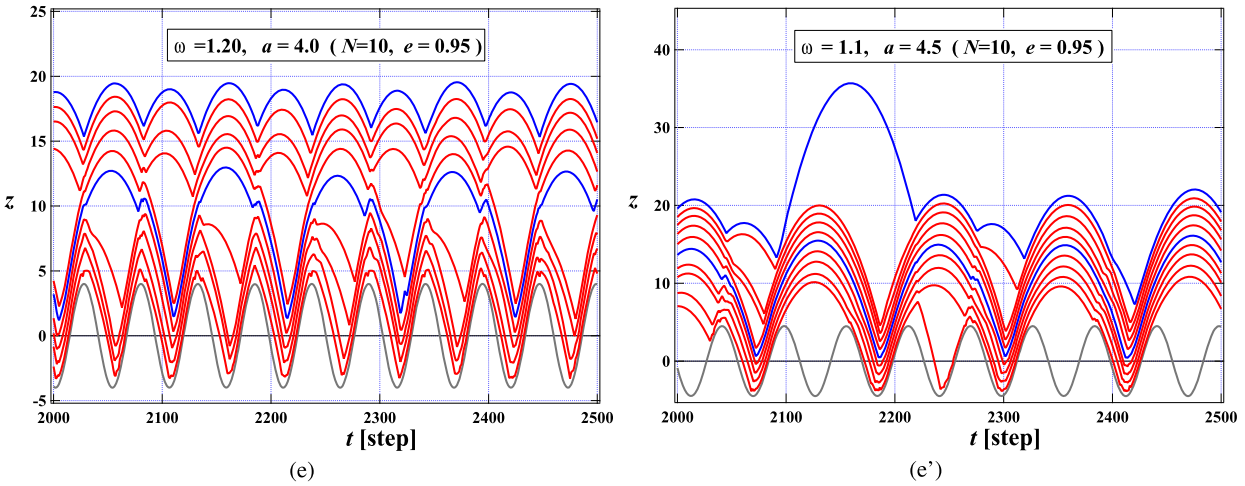

Fig. 3. (*continued*)

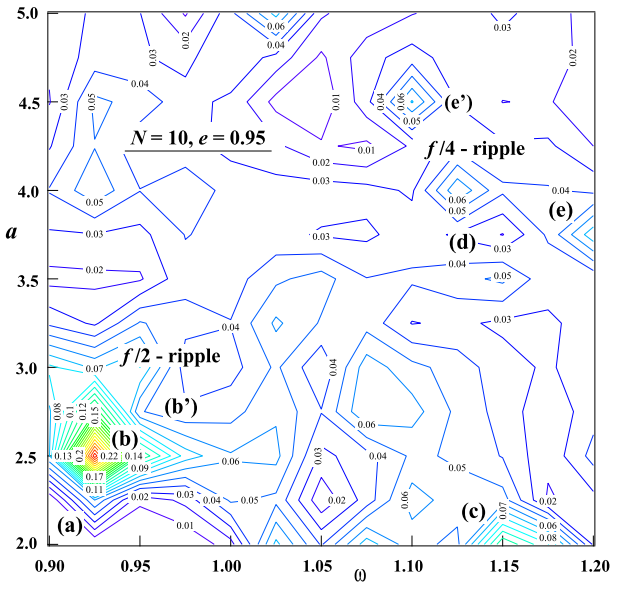

Fig. 4. (Color online.) Contour map β in the ω–a plane with $N = 10$ and $e = 0.95$.

state is maintained as a first approximation, so that p and ρ^* are almost constant in the bulk region at the instant of the collision [41,42], so that $K^* \propto 1/\Delta$, which determines ν.

An event-driven numerical calculation was carried out in our model system starting with a given initial condition, where a time step was chosen as $\Delta t = 10^{-3}$. Particles are assumed to move freely under the gravity force when they are isolated from each other. For collisions, which occur for $|z_{i+1} - z_i| \leqslant d$ (in the case of the collision of the lowest particle to the bottom wall, this condition is $|z_1 - z_0| \leqslant d/2$), we interpolated the exact time of collision, applied Eqs. (3) and (4), and calculated the positions and velocities of the particles i and $i+1$ after one time step Δt. The average positions and their standard deviations after sufficient time has passed were obtained over the time interval of about $100T$, where T is the period of oscillation of the bottom wall. To do this, we assumed the relation $v \propto \exp(-\beta z/2)$, and calculated the best fit of the coefficient β for the numerical data for the particles numbered $i = 3$ to $N - 2$ in each column. Here we have omitted a few particles on both sides of the column, because the lower part depends strongly on the motion of the bottom wall, whereas the upper part of the particles moves almost freely during considerable time so that it would not be appropriated to regard it as a part of the continuum. The dependence of the wavelength λ (or β) on the number of particles N, the restitution coefficients e, e', the external forcing frequency f and the amplitude a are examined.

In the following numerical simulation, however, we shall show the results obtained for $e = e' = 0.95$ in order to shed light on the dependence on N. Fig. 3 shows some typical behavior of particles in the $N = 10$ case. For the lower values of f and a, all the particles in the column move up and down in a cluster with a period T of oscillation of the bottom

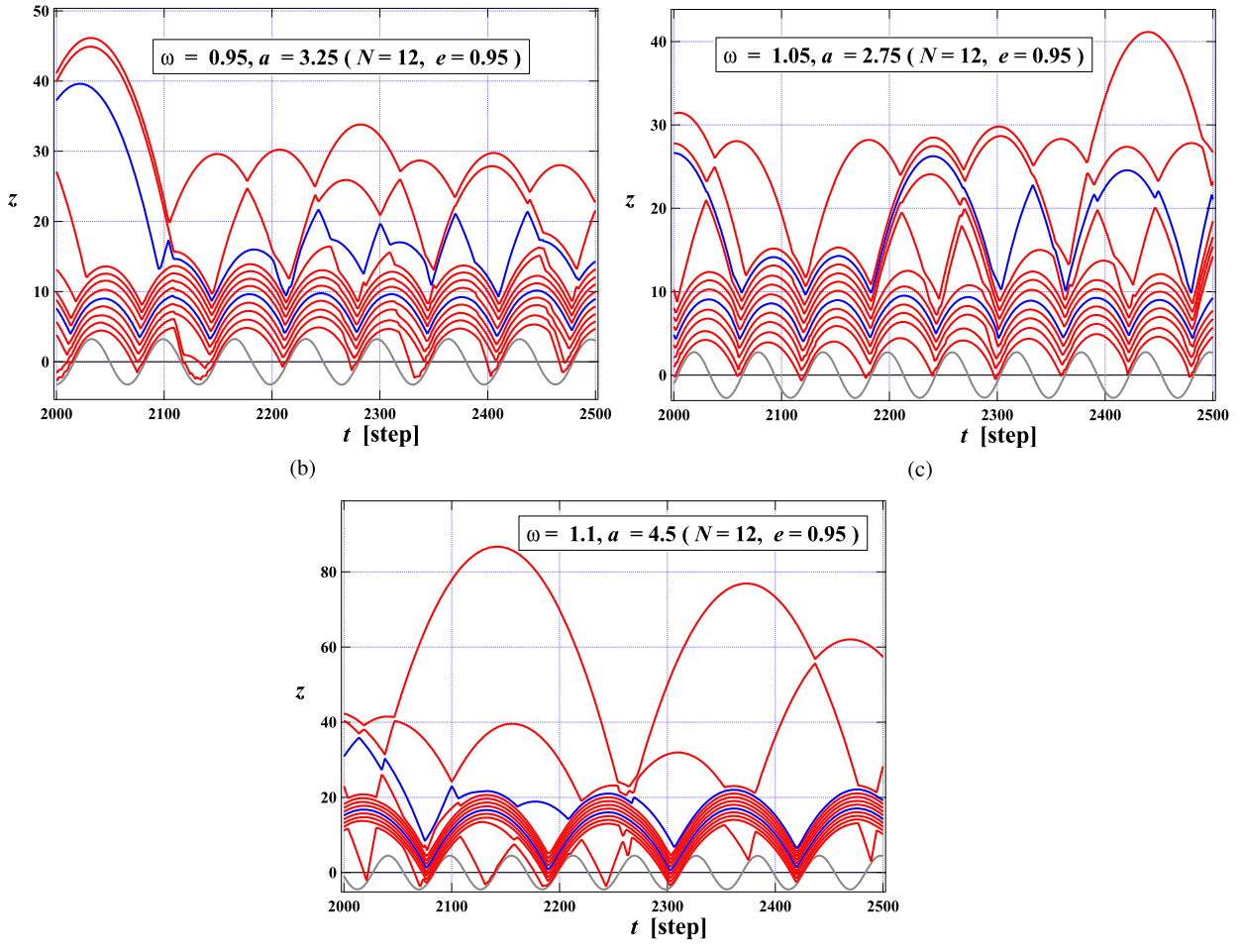

Fig. 5. (Color online.) Particle behavior for $N = 12$; $(\omega, a) =$ (b) $(0.950, 3.25)$, (c) $(1.050, 2.75)$, and (e) $(1.100, 4.50)$. Regular motion is recognized in (a) and (d) in the contour map of Fig. 6. In (b), (c) and (e), the lower part of the layer is almost solid-like, but the dilatation looks larger in the upper layers. Sometimes the separation of the layer in the middle part is recognized.

wall, as shown in Fig. 3(a). As the acceleration is increased, the amplitudes of the motion in the upper part of the particles increase, either periodically (Fig. 3(b)) or aperiodically (Figs. 3(b′)(c)), whereas the particles in the lower part of the layer move almost periodically in clusters. When acceleration increases, all the particles in the column move again in a cluster with a period twice as long as the external oscillation $2T$ (Fig. 3(d)). When acceleration further increases, the particles in the column sometimes split into two clusters, as shown in Fig. 3(e), or sometimes move irregularly, as shown in Fig. 3(e′), but their behaviors are mainly characterized by the period $2T$. (We have not examined the particle behavior under much higher frequency, but it may be possible to have a periodic motion with $3T$ or more.) Fig. 4 shows the contour map of β for $N = 10$ as a function of f $(= \omega/(2\pi))$ and a. Figs. 5 and 7 show some examples of the particle behavior in the $N = 12$ and $N = 14$ cases, respectively. Periodic motions in a cluster as shown in Figs. 3(a) and (d) are also observed in all cases, which are marked in the corresponding contour maps Figs. 6 and 8, respectively. In each contour map, we can recognize the local maxima of β distributed around a curve ranging from "smaller f and larger a" to "larger f and smaller a". The positions of these local maxima seem to shift to larger a and f values as the particles' number N increases.

Fig. 9 shows the position of the local maxima of β in ω–a plane. We also plotted experimental data (Fig. 4 of Ref. [11]), where the same normalization adopted here is taken, so that the abscissa is the angular frequency $2\pi f\sqrt{d/g}$, and the ordinate is a/d. Experimental data are based on spherical lead beads of a diameter $d = 1$ mm or 2 mm, as shown in the figure. Here, the layer is in a fully fluid-like state, so that the macroscopic scaling $h \approx Nd$ is relevant, e.g., data for 10 layers of particles with $d = 1$ mm and those for 5 layers of particles with $d = 2$ mm overlap in the ω–a plane. Compared with the experimental data, the present numerical results show a slight shift to lower values of a and ω. This is probably because the motion of the particle is restricted to one dimension in the present numerical model, whereas much larger energy dissipation associated with 3D collisions occurs in the experiment. In spite of larger variations, the shift of local maxima toward larger $a\omega$ values with the increase of the layer number is recognized in the $f/2$ ripple.

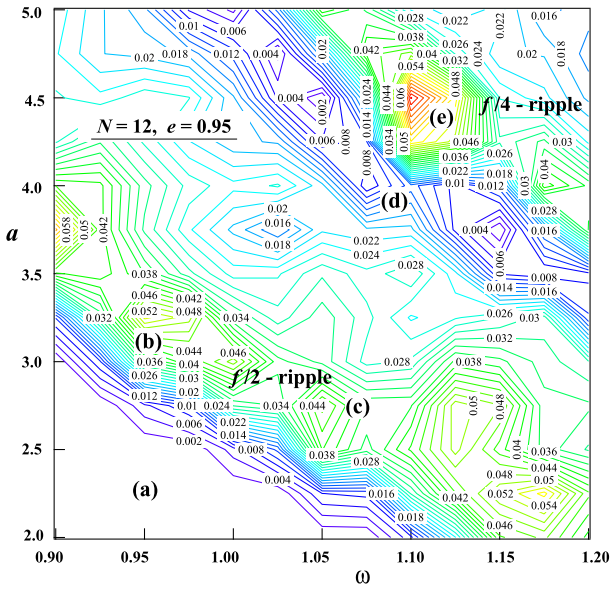

Fig. 6. (Color online.) Contour map β in the ω–a plane with $N = 12$ and $e = 0.95$.

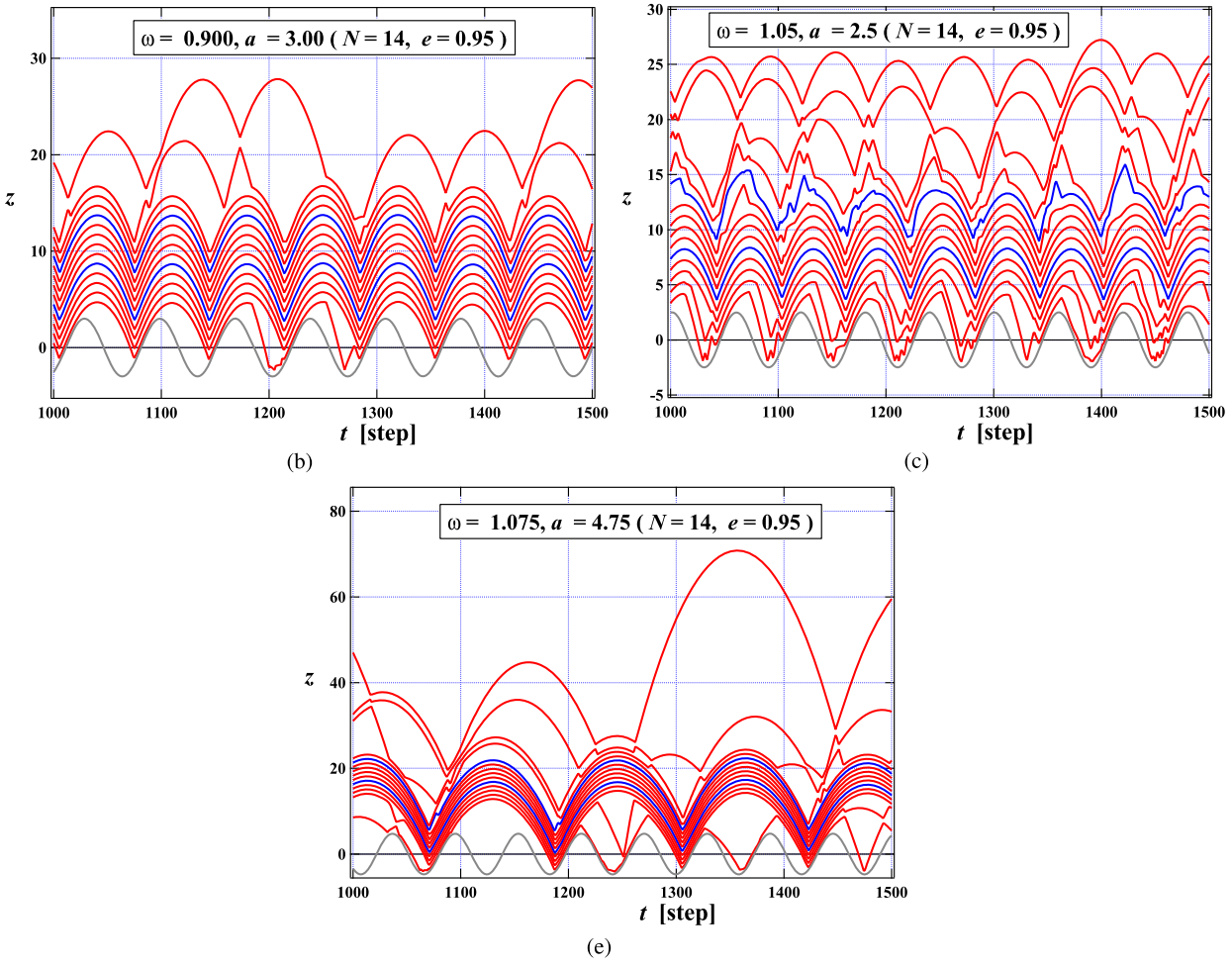

Fig. 7. (Color online.) Particle behavior for $N = 14$; (ω, a) = (b) $(0.900, 3.00)$, (c) $(1.05, 2.50)$, and (e) $(1.075, 4.75)$. Regular motion is recognized in (a) and (d) in the contour map Fig. 8. In (b), (c) and (e), the lower part of the layer is almost solid-like, but the dilatation looks larger in the upper layers. Sometimes the separation of the layer in the middle part is recognized.

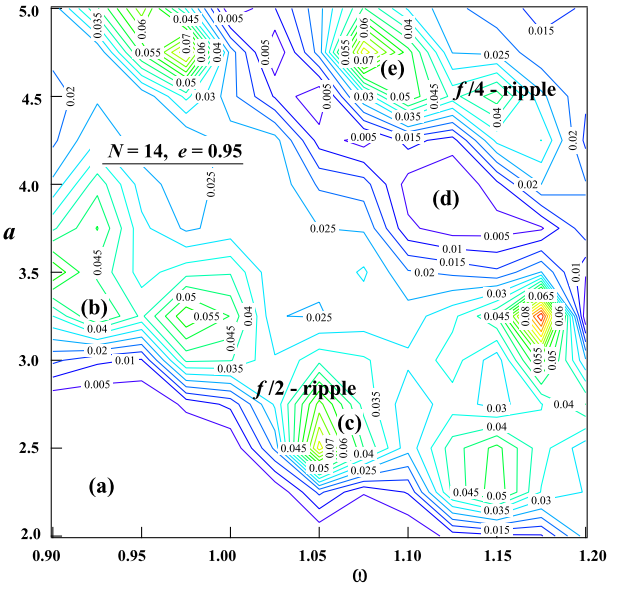

Fig. 8. (Color online.) Contour map β in the ω–a plane with $N = 14$ and $e = 0.95$.

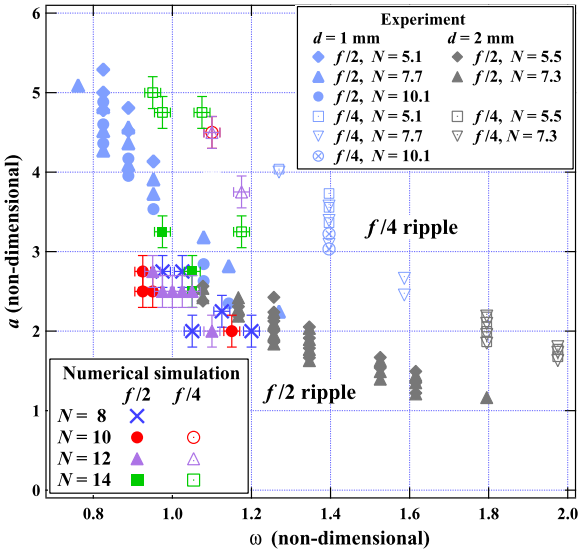

Fig. 9. (Color online.) Pattern diagram of the observed $f/2$-ripples and $f/4$-ripples.

Although the present simulation is limited to the one-dimensional motion of the column of beads, some symptom can be seen by a smaller shift of the emergence region between the $N = 12$ and the $N = 14$ cases, which supports the experimental findings that the lower part of the dynamically thick layer is immobilized and only the upper part of the layer is responsible for surface deformation, so that the wavelength of the ripple is mainly determined by the upper fluidized part. The lower immobilized part mainly transmits the momentum given at the collision with the container bottom to the upper fluidized part, which explains the saturation of the wavelength with respect to the layer's thickness (Fig. 10).

3. Concluding remarks

We have performed a numerical simulation of the column of particles under vertical oscillation. Multiple collisions among particles reveal a time-dependent distribution of particles, which reflects a propagation velocity v similar to the one known in the theory of elasticity. Our numerical simulation shows that the dependence of v on the vertical height z is well approximated by $v \propto \exp(-\beta z/2)$ near the surface.

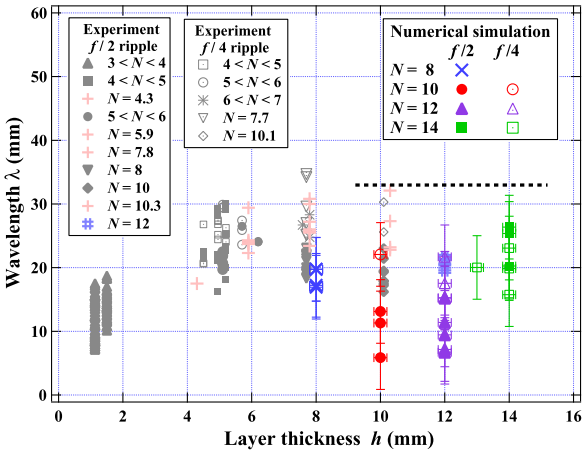

Fig. 10. (Color online.) Dispersion relation for $f/2$-ripples and $f/4$-ripples. Wavelength saturates for dynamically thick layers.

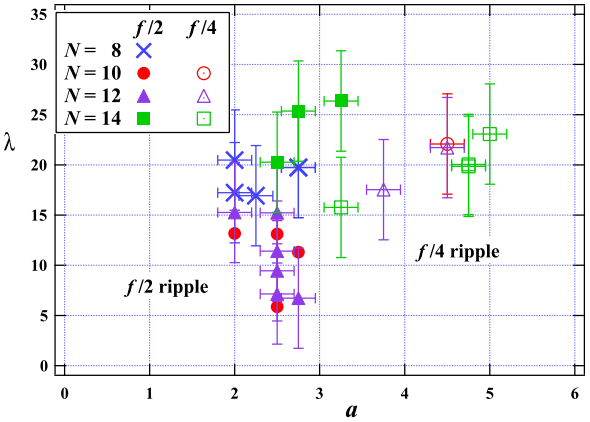

Fig. 11. (Color online.) Dependence of amplitude a on wavelength λ.

If we apply the present theory to a quasi-two-dimensional dynamically thick granular layer, a disturbance will be transmitted faster in the lower compacted part of the layer, whereas it will be transmitted slower in the upper loosely contacting part of the layer, so that the number density non-uniformity will be propagated upward as it travels horizontally [41,42]. The latter spatiotemporal change is observed as a density wave refraction, which is described by the "ray" theory. In our theory, the magnitude of refraction is determined by the change of particle distribution β, and not the distribution itself, so that the dispersion relation is not directly affected by the layer thickness h. Under given f and a, a wavelength corresponding to the nearest local maximum β is chosen, because the shorter wavelength crests look dominant over a longer smooth surface. As mentioned in the previous section, local maxima of β are distributed around two curves ranging from "smaller f and larger a" to "larger f and smaller a", as shown in Fig. 9, and taking into account that the two groups consists of the particle motion of period T and $2T$ (or period $2T$ and $4T$ for pattern repetition), these maxima are considered to be the emergence region of $f/2$-ripples or $f/4$-ripples, in agreement with those observed in the experiment. As the layer thickness is increased, the emergence region appears to shift to larger f and larger a areas.

Figs. 11 and 12 show the dependence of the wavelength λ calculated by Eq. (2) on a and $a\omega$, respectively. Compared with the former, the latter has smaller variations. The data points for $f/2$-ripple are well approximated by a straight line $\lambda = -30.418 + 17.378a\omega$, showing the presence of the critical value $(a\omega)_c \approx 1.75$ for the emergence of ripples, which may depend on e, or other properties of particles. We also show the least-square fit of the $f/4$-ripple data, such that it passes the point $(a\omega)_c \approx 1.75$ by the broken line in Fig. 12. Rather good scaling of λ/d on the momentum $a\omega \propto mv$, and not on $\Gamma \equiv a\omega^2/g$ nor $f\sqrt{h/g}$ (h being the layer thickness) should be remarked.

Note that f and a values have considerable error bars associated with fitting the numerical simulation to the relation $v \propto \exp(-\beta z/2)$. A larger variation, however, reflects a larger adjustability to the externally applied oscillation conditions. Indeed we have observed experimentally the adjustment of the size and shape of the fluid-like domain to keep the ripple motion, whereas the residual energy is given to the immobilized domain [41–43]. The dependence of β on other properties of the particle, like friction, density, and restitution coefficient, is left for clarification in our future investigations.

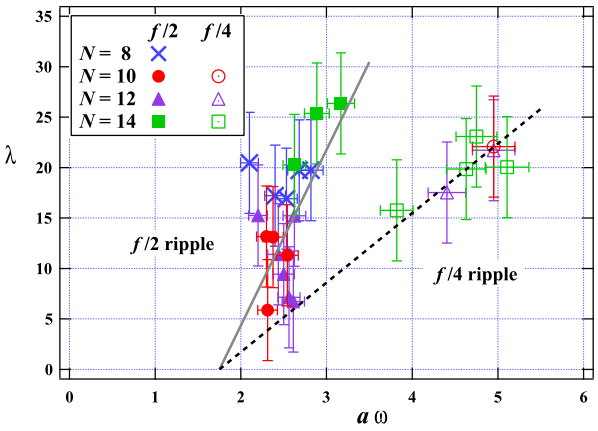

Fig. 12. (Color online.) Dependence of $a\omega$ on λ.

Acknowledgement

This work was partially supported by a Grant-in-Aid for Scientific Research (C) from the Ministry of Education, Culture, Sports, Science and Technology, Japan.

References

[1] M. Faraday, On a peculiar class of acoustical figures; and on certain forms assumed by groups of particles upon vibrating elastic surfaces, Philos. Trans. R. Soc. Lond. 121 (1831) 299.
[2] H.M. Jaeger, S.R. Nagel, Physics of the granular state, Science 255 (1992) 1523.
[3] H.M. Jaeger, S.R. Nagel, R.P. Behringer, Granular solids, liquids, and gases, Rev. Mod. Phys. 68 (1996) 1259.
[4] M.C. Cross, P.C. Hohenberg, Pattern formation outside of equilibrium, Rev. Mod. Phys. 65 (1993) 851.
[5] I.S. Aranson, L.S. Tsimring, Patterns and collective behavior in granular media: Theoretical concepts, Rev. Mod. Phys. 78 (2006) 641.
[6] S. Douady, S. Fauve, C. Laroche, Subharmonic instabilities and defects in a granular layer under vertical vibrations, Europhys. Lett. 8 (1989) 621–627.
[7] A. Goldshtein, M. Shapiro, L. Moldavsky, M. Fichman, Mechanics of collisional motion of granular materials. Part 2. Wave propagation through vibrofluidized granular layers, J. Fluid Mech. 287 (1995) 349–382.
[8] Y. Lan, A.D. Rosato, Convection related phenomena in granular dynamics simulations of vibrated beds, Phys. Fluids 9 (1997) 3615–3624.
[9] K.A. Aoki, T. Akiyama, K. Yamamoto, T. Yoshikawa, Experimental study on the mechanism of convection modes in vibrated granular beds, Europhys. Lett. 40 (1997) 159–164.
[10] A. Ugawa, O. Sano, Undulation of a thin granular layer induced by vertical vibration, J. Phys. Soc. Jpn. 72 (2003) 1390–1395.
[11] K. Kanai, A. Ugawa, O. Sano, Experiment on vibration-induced pattern formation of a vertically thin granular layer, J. Phys. Soc. Jpn. 74 (2005) 1457–1463.
[12] O. Sano, Dilatancy, buckling, and undulations on a vertically vibrating granular layer, Phys. Rev. E 72 (2005) 051302-1-7.
[13] P. Eshuis, Ko van der Weele, Devaraj van der Meer, R. Bos, D. Lohse, Phase diagram of vertically shaken granular matter, Phys. Fluids 19 (2007) 123301-1-11.
[14] F. Melo, P. Umbanhowar, H.L. Swinney, Transition to parametric wave patterns in a vertically oscillated granular layer, Phys. Rev. Lett. 72 (1994) 172–175.
[15] E. Clément, L. Vanel, J. Rajchenbach, J. Duran, Pattern formation in a vibrated granular layer, Phys. Rev. E 53 (1996) 2972–2975.
[16] S. Luding, E. Clément, J. Rajchenbach, J. Duran, Simulations of pattern formation in vibrated granular media, Europhys. Lett. 36 (1996) 247–252.
[17] K.M. Aoki, T. Akiyama, Spontaneous wave pattern formation in vibrated granular materials, Phys. Rev. Lett. 77 (1996) 4166–4169.
[18] E. Clément, L. Labous, Pattern formation in a vibrated granular layer: The pattern selection issue, Phys. Rev. E 62 (2000) 8314–8323.
[19] A. Ugawa, O. Sano, Dispersion relation of standing waves on a vertically oscillated thin granular layer, J. Phys. Soc. Jpn. 71 (2002) 2815–2819.
[20] F. Melo, P.B. Umbanhowar, H.L. Swinney, Hexagons, kinks, and disorder in oscillated granular layers, Phys. Rev. Lett. 75 (1995) 3838–3841.
[21] P.B. Umbanhowar, F. Melo, H.L. Swinney, Localized excitations in a vertically vibrated granular layer, Nature 382 (1996) 793–796.
[22] T.H. Metcalf, J.B. Knight, H. Jaeger, Standing wave patterns in shallow beds of vibrated granular material, Physica A 236 (1997) 202–210.
[23] C. Bizon, M.D. Shattuck, J.B. Swift, W.D. McCormick, H.L. Swinney, Patterns in 3D vertically oscillated granular layers: simulation and experiment, Phys. Rev. Lett. 80 (1998) 57–60.
[24] O. Sano, A. Ugawa, K. Suzuki, Pattern formation on the vertically vibrated granular layer, Forma 14 (1999) 321–329.
[25] P.B. Umbanhowar, F. Melo, H.L. Swinney, Periodic, aperiodic, and transient patterns in vibrated granular layers, Physica A 249 (2000) 1–9.
[26] P.B. Umbanhowar, H.L. Swinney, Wavelength scaling and square/stripe and grain mobility transitions in vertically oscillated granular layers, Physica A 288 (2000) 344–362.
[27] L.S. Tsimring, I.S. Aranson, Localized and cellular patterns in a vibrated granular layer, Phys. Rev. Lett. 79 (1997) 213.
[28] E. Cerda, F. Melo, S. Rica, Model for subharmonic waves in granular materials, Phys. Rev. Lett. 79 (1997) 4570–4573.
[29] D. Blair, I.S. Aranson, G.W. Crabtree, V. Vinokur, L.S. Tsimring, C. Josserand, Patterns in thin vibrated granular layers: Interfaces, hexagons, and superoscillons, Phys. Rev. E 61 (2000) 5600.
[30] J. Bougie, J. Kreft, J.B. Swift, H.L. Swinney, Onset of patterns in an oscillated granular layers: Continuum and molecular dynamic simulations, Phys. Rev. E 71 (2005) 021301-1-9.
[31] C. Bizon, M.D. Shattuck, J.B. Swift, Linear stability analysis of a vertically oscillated granular layer, Phys. Rev. E 60 (1999) 7210.
[32] J.D. Goddard, A.K. Didwania, A fluid-like model of vibrated granular layers: Linear stability, kinks, and oscillons, Mech. Mater. 41 (2009) 637–651.
[33] E.C. Rericha, C. Bizon, M.D. Shattuck, H.L. Swinney, Shocks in supersonic sand, Phys. Rev. Lett. 88 (2002) 014302-1-4.
[34] J. Bougie, S.-J. Moon, J.B. Swift, H.L. Swinney, Shocks in vertically oscillated granular layers, Phys. Rev. E 66 (2002) 051301-1-9.

[35] K. Huang, G. Miao, P. Zhang, Y. Yun, R. Wei, Shock wave propagation in vibrofluidized granular materials, Phys. Rev. E 73 (2006) 041302-1-5.
[36] S.-J. Moon, M.D. Shattuck, C. Bizon, D.I. Goldman, J.B. Swift, H.L. Swinney, Phase bubbles and spatiotemporal chaos in granular patterns, Phys. Rev. E 65 (2002) 011301-1-10.
[37] S.-J. Moon, D.I. Goldman, J.B. Swift, H.L. Swinney, Kink-induced transport and segregation in oscillated granular layers, Phys. Rev. Lett. 91 (2003) 134301-1-4.
[38] N. Mujica, F. Melo, Solid–liquid transition and hydrodynamic surface waves in vibrated granular layers, Phys. Rev. Lett. 80 (1998) 5121–5124.
[39] M.D. Sinnott, P.W. Cleary, Vibration-induced arching in a deep granular bed, Granul. Matter 11 (2009) 345–364.
[40] O. Sano, A. Takei, A density wave in a vertically vibrating granular layer and the occurrence of spikes and ripples on its surface, AIP Conf. Proc. 1145 (2009) 729–732.
[41] O. Sano, Solid–fluid transition and the formation of ripples in vertically oscillated granular layers, AIP Conf. Proc. 1227 (2010) 100–114.
[42] O. Sano, Density wave as a mechanism of the formation of ripples in vertically oscillated granular layer, J. Phys. Soc. Jpn. 80 (2011) 034402-1-7.
[43] O. Sano, Wavelength selection mechanism of ripples in vertically vibrated thicker granular layer, J. Phys. Soc. Jpn. 81 (2012) 033401-1-4.
[44] S. McNamara, W.R. Young, Inelastic collapse and clumping in a one-dimensional granular medium, Phys. Fluids A, Fluid Dyn. 4 (1992) 496–504.
[45] I. Goldhirsch, G. Zanetti, Clustering instability in dissipative gases, Phys. Rev. Lett. 70 (1993) 1619–1622.
[46] J.M. Luck, A. Mehta, Bouncing ball with a finite restitution: Chattering, locking, and chaos, Phys. Rev. E 48 (1933) 3988–3997.
[47] S. Luding, E. Clément, A. Blumen, J. Rajchenbach, J. Duran, Studies of columns of beads under external vibrations, Phys. Rev. E 49 (1994) 1634–1646.
[48] S. Luding, E.H.J. Herrmann, A. Blumen, Simulations of two-dimensional arrays of beads under external vibrations: Scaling behavior, Phys. Rev. E 50 (1994) 3100–3108.
[49] B. Bernu, F. Delyon, R. Mazighi, Steady states of a column of shaken inelastic beads, Phys. Rev. E 50 (1994) 4551–4559.
[50] L.D. Landau, E.M. Lifshitz, Theory of Elasticity, Pergamon, Oxford, 1986.